



Article

Increase in Soil Carbon Pool Stability Rather Than Its Stock in Coastal Saline—Alkali Ditches following Reclamation Time

Xiangrong Li ^{1,2,†}, Zhen Liu ^{1,3,*,†} , Jing Li ^{1,3}, Huarui Gong ^{1,3} , Yitao Zhang ^{1,3}, Zhigang Sun ^{1,3} and Zhu Ouyang ^{1,3}

¹ CAS Engineering Laboratory for Yellow River Delta Modern Agriculture, Institute of Geographic Sciences and Natural Resources Research, Chinese Academy of Sciences, Beijing 100101, China; lxr2021@nwfau.edu.cn (X.L.); jingli@igsnr.ac.cn (J.L.); gonghr.18b@igsnr.ac.cn (H.G.); zhangyt@igsnr.ac.cn (Y.Z.); sun.zhigang@igsnr.ac.cn (Z.S.); yes@igsnr.ac.cn (Z.O.)

² State Key Laboratory of Soil Erosion and Dryland Farming on the Loess Plateau, Northwest A&F University, Yangling 712100, China

³ Shandong Dongying Institute of Geographic Sciences, Dongying 257000, China

* Correspondence: liuzhen@igsnr.ac.cn

† These authors contributed equally to this work.

Abstract: Extensive drainage ditches are constructed to reduce soil salinity in reclaimed saline–alkali farmland, consequently forming plant growth hotspots and impacting soil carbon stocks therein. However, the investigation into changes in soil carbon stocks remains limited in these ditches. To address this, soil samples were collected from drainage ditches, which originated from the reclamation of saline–alkali farmland, at different reclamation years (the first, seventh, and fifteenth year). Moreover, fractions were separated from soil samples; a particle size separation method (particulate organic matter, POM; mineral-associated organic matter, MAOM) and a spatio-temporal substitution method were conducted to analyze the variations in soil carbon components and the underlying mechanisms. The results indicate that there were no significant variations in the contents and stocks of soil organic carbon (SOC) and soil inorganic carbon (SIC) following the increase in reclamation time. However, in the POM fraction, the SOC content (SOC_{POM}) and stock significantly decreased from 2.24 to 1.12 g kg^{−1} and from 19.02 to 12.71 Mg ha^{−1}, respectively. Conversely, in the MAOM fraction, the SOC content (SOC_{MAOM}) and stock significantly increased from 0.65 to 1.70 g kg^{−1} and from 5.30 to 12.27 Mg ha^{−1}, respectively. The different changes in SOC_{POM} and SOC_{MAOM}, as well as the result of the structural equation model, showed a possible transformation process from SOC_{POM} to SOC_{MAOM} in the soil carbon pool under the driving force of reclamation time. The results in terms of the changes in soil carbon components demonstrate the stability rather than the stock of the soil carbon pool increase in coastal saline–alkali ditches following the excavation formation time. Although more long time series and direct evidence are needed, our findings further provide a case study for new knowledge about changes in the soil carbon pool within saline–alkali ditches and reveal the potential processes involved in the transformation of soil carbon components.

Keywords: soil carbon pool; saline–alkali ditches; coastal soils; soil carbon components; carbon stability



Citation: Li, X.; Liu, Z.; Li, J.; Gong, H.; Zhang, Y.; Sun, Z.; Ouyang, Z. Increase in Soil Carbon Pool Stability Rather Than Its Stock in Coastal Saline—Alkali Ditches following Reclamation Time. *Agronomy* **2023**, *13*, 2843. <https://doi.org/10.3390/agronomy13112843>

Academic Editor: Liyin Liang

Received: 7 October 2023

Revised: 8 November 2023

Accepted: 17 November 2023

Published: 19 November 2023



Copyright: © 2023 by the authors. Licensee MDPI, Basel, Switzerland. This article is an open access article distributed under the terms and conditions of the Creative Commons Attribution (CC BY) license (<https://creativecommons.org/licenses/by/4.0/>).

1. Introduction

The soil carbon pool is the largest carbon pool in terrestrial ecosystems, composed primarily of soil organic carbon (SOC) and soil inorganic carbon (SIC) [1,2]. Changes in its stock have significant implications for global carbon cycling and climate change [3,4]. The soil carbon pool is influenced by natural factors such as vegetation, soil quality, temperature, and precipitation [1,5]. However, the significant impact of human activities, such as land management and land use changes, on the soil carbon pool should not be underestimated [4,6], particularly in the land use change after reclamation. For example, the irrational process of land reclamation disrupts soil aggregations [7], thereby affecting

plant root growth and microbial activity [8], ultimately leading to a significant decrease in SOC and soil nutrient content [9]. Therefore, investigations into the changes in soil carbon pools are crucial for formulating rational land management strategies, as well as for regulating the soil carbon stocks.

Divergence variations in soil carbon pools after land reclamation have been exhibited in the recent studies. It is characterized by significant increases [10,11], significant decreases [12], and decreases, followed by increases in SOC content [13]. Furthermore, SIC content slightly increases with shorter reclamation times and decreases with longer reclamation times [11]. Similar trends are observed in carbon stocks after reclamation [14,15]. These inconsistencies are primarily due to the variations in soil types and vegetation types among the various experimental conditions, as well as the complex interactions between SOC and SIC. Generally, the stock of the soil carbon pool relies on a balance between the formation of SOC from plant residues and the mineralization of SOC [16]. Plant residues and root exudates are crucial sources of SOC, thereby rendering the changes in the soil carbon pool easily influenced by vegetation conditions after reclamation, e.g., plant biomass and diversity after reclamation [17,18]. Previous research has focused on driving factors impacting the soil carbon pool, such as reclamation time and land use type [13,19]. However, investigating the changes in different soil carbon components and the mechanisms of SOC to SIC pool transformation remains limited, which hinders a deeper understanding of the processes and mechanisms of soil carbon stock changes therein.

Soil organic matter (SOM) is directly related to SOC and influences the stability of the changes in soil carbon pools [20,21]. Due to the complexity of SOM, characterizing the different fractions of SOM has become a conventional technique for revealing its transformation processes [22–24]. SOM is commonly categorized into two fractions: particulate organic matter (POM) and mineral-associated organic matter (MAOM), based on its size or density [25–28]. POM primarily originates from plant residues [29,30], while MAOM is mainly derived from microbial metabolites [31,32]. However, recent research suggests that soluble organic compounds also directly contribute to the formation of MAOM [16,33]. Some studies suggest that the decomposition of POM generates soluble organic compounds which directly contribute to MAOM formation, thus linking POM and MAOM [28]. Other studies propose that the formation of MAOM is independent of POM and relies on the input of soluble compounds from plant residues [34,35]. Due to the complex relationship between POM and MAOM, previous investigation has attempted to quantify the association between POM and MAOM fractions with SOC or soil total carbon (TC) [27]. However, few studies have examined the relationship between SIC and POM or MAOM fractions, as well as their potential transformations. Therefore, it is necessary to fully consider the changes in SOC and SIC of POM and MAOM fractions and investigate their transformation mechanisms.

The Yellow River Delta is formed by the sediment of the Yellow River. It is primarily comprised of coastal saline–alkali soil as a result of intense land–sea interactions [36]. In recent years, the construction of numerous drainage ditches has been carried out to reduce soil salinity during land reclamation, with the unutilized land accounting for 9.10% or more of the total farmland area [37]. The specific conditions of drainage ditches can impact soil carbon stocks. For example, waterlogging resulting from drainage alters the structure of soil microbial communities, inhibits microbial activity, and reduces the rate of SOM decomposition and mineralization [11,38–41]. Moreover, the accumulation of soil salinity in drainage ditches may restrict plant growth and microbial activities, thereby affecting changes in SOC stock and stability [42]. Conversely, the unique structure of drainage ditches promotes material exchange and creates an improved saline–alkali environment, leading to the formation of plant growth hotspots. Considering the changes in the amount of carbon input by plants into the soil and the rate of SOM mineralization influenced by microbial activity, the presence of ditches can significantly influence the original soil carbon stocks and stability. The extent of salt-affected land in the Yellow River Delta region is

approximately 240,000 ha [43]. If all of them were reclaimed as saline–alkali farmland with drainage ditches, the changes in soil carbon stock should not be underestimated.

Therefore, the objective of this study is to investigate the processes and transformation mechanisms of changes in soil carbon stocks within saline–alkali ditches formed by farmland reclamation in the Yellow River Delta. We measured the carbon content and physicochemical properties of the drainage ditch soils in saline–alkali farmland after different reclamation times (the first, seventh, and fifteenth year). Furthermore, we attempted to explore the processes and mechanisms of changes in soil carbon components by separating POM and MAOM fractions. The present study provides a theoretical foundation for managing the soil carbon pool in recovered saline–alkali areas.

2. Materials and Methods

2.1. Site Description

This research was conducted at the Yellow River Delta Research Center, Chinese Academy of Sciences, in Dongying, Shandong Province, China (37°40'N, 118°55' E). The study area is situated in the alluvial deposition zone of the Yellow River Delta, characterized by saline–alkali soils. The area experiences a temperate continental monsoon climate, with an average annual temperature of 12.40 °C. The annual average precipitation ranges from 530–630 mm, with the majority occurring between June and September. Additionally, the annual evaporation is 1962 mm. Over recent years, extensive land development has occurred, resulting in the creation of numerous drainage ditches (Figure 1). The soil in this region has originated from the sediment of the Yellow River since 1855, and the main soil type is Calcaric Fluvisols, comprising 5.90% caly, 70.88% silt, and 23.22% sand. The vegetation in these drainage ditches primarily comprises reed (*Phragmites australis* (Cav.) Trin. ex Steud.), Suaeda salsa (*Suaeda salsa* (L.) Pall.), Imperata cylindrica (*Imperata cylindrica* (L.) P. Beauv.), Leymus chinensis (*Leymus chinensis* (Trin.), and Artemisia capillaris (*Artemisia capillaris* Thunb.).

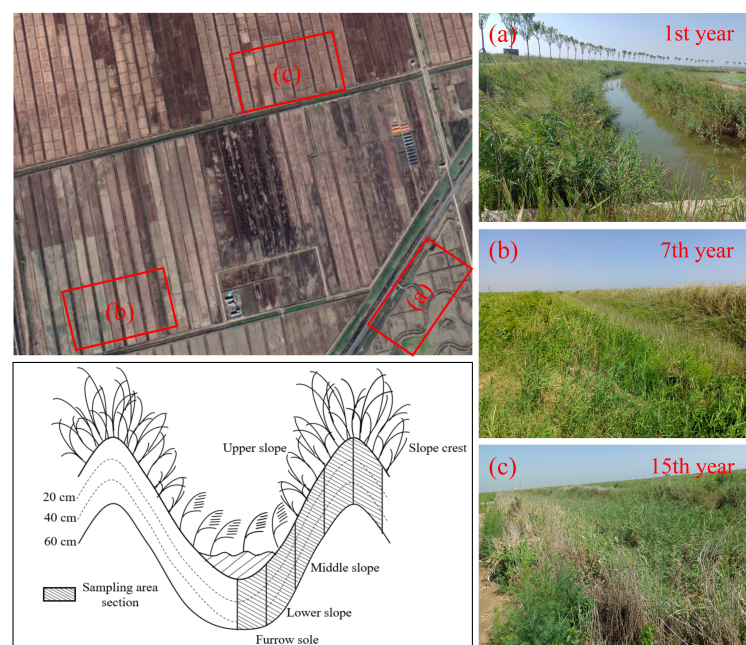


Figure 1. Distribution of sampling sites in the study area and the schematic diagram of the saline–alkali ditch.

2.2. Soil Sampling Collection

To investigate the changes in soil carbon stocks of saline–alkali ditches, three 1 km × 1 km sampling sites with different reclamation years, including the 1st, 7th, and 15th year, were

selected in the saline–alkali farmland within a distance of 2 km from each other. Within each sampling site, four drainage ditches adjacent the farmlands were selected as sampling plots which had similar cross–section dimensions, ditch length, and vegetation coverage. Furthermore, within each sampling plot, three slope cross–sections were randomly selected. In each cross–section, five 1 m × 1 m subplots on the different positions, including the upper slope, middle slope, lower slope, slope crest, and furrow sole, were selected to collect the samples (Figure 1). For each subplot, we measured the height of the plants and assessed the vegetation coverage. Subsequently, all aboveground plants in the subplot were collected to evaluate the biomass. The vegetation coverage and growth conditions for sampling plots with the same reclamation year are presented in Table S1. Soil samples at depths of 0–20 cm, 20–40 cm, and 40–60 cm were collected using a soil auger. Due to the complex water and soil conditions in the furrow sole, soil samples were taken at depths of 0–20 cm and 20–40 cm. Soil samples obtained from the corresponding position and depth in the three slope sections of each plot were mixed to create a representative sample. In total, 168 composite samples were obtained. The mixed soil sample were sieved using a 2 mm mesh to remove plant debris and divided into two portions. The first portion, 500 g, was air–dried and used to measure soil parameters, including TC, SIC, SOC, POM, MAOM, soil total nitrogen (TN), soil total phosphorus (TP), soil available phosphorus (AP), soil pH, and soil electrical conductivity (EC). Moreover, to obtain the fractions of POM and MAOM, a particle size separation method was employed [25,44]. Specifically, 10 g of the air–dried soil was dispersed in 30 mL of 5 g L^{−1} sodium hexametaphosphate via shaking for 15 h on a reciprocal shaker. The dispersed soil samples were passed through a 53 μm sieve and, after rinsing several times with water, the material that was retained on the sieve was defined as POM fraction (53–2000 μm) and the material passing through the sieve (<53 μm) was labeled as MAOM fraction. The divided soil was further utilized to determine the content of organic carbon (SOC_{POM}) and inorganic carbon (SIC_{POM}) in POM fraction soil, as well as organic carbon (SOC_{MAOM}) and inorganic carbon (SIC_{MAOM}) in MAOM fraction soil. The second portion, weighing 300 g, was stored at 4 °C and used to measure soil water content (SWC), soil dissolved organic carbon (DOC), soil soluble ammonium nitrogen (NH₄⁺-N), and soil soluble nitrate nitrogen (NO₃[−]-N).

2.3. Soil Sample Processing

TC and SIC contents were analyzed using an automated carbon–nitrogen analyzer (Primacs SNC100–IC–E, Skalar Analytical BV, Breda, The Netherlands). TC content was determined based on high–temperature combustion and non–dispersive infrared detection (NDIR), while SIC content was obtained via automatic acidification heating, gas purging, and non–dispersive infrared detection (NDIR). SOC content was calculated by subtracting SIC content from TC content. AP content was measured using a continuous flow analyzer (Auto Analyzer 3, Bran and Luebbe GmbH, Norderstedt, Germany). Soil pH and EC values were determined by a soil–water mixture with a ratio of 1:5. Soil pH was measured using a pH meter (PHS–3E, Leici Instruments, Shanghai, China) and EC was measured using an electrical conductivity meter (FE38–Standar, Mettler Toledo, Greifensee, Switzerland). TN content was determined using the Kjeldahl method, while TP content was determined using the H₂SO₄–HClO₄ digestion method. Both TN and TP were measured using the continuous flow analyzer. DOC content was determined using the method developed by Zhan and Zhou [45]. NH₄⁺-N and NO₃[−]-N contents were determined using the KCl–indophenol blue colorimetric method and the dual–wavelength UV–Visible spectrophotometric method, respectively.

2.4. Calculation of Soil Carbon Stocks

The SOC and SIC stocks at different slope sampling positions are calculated according to Liu et al. [46] as follows:

$$M_{\text{SOC}} = 0.1 \times D \times B \times C_{\text{SOC}} \times K \quad (1)$$

$$M_{SIC} = 0.1 \times D \times B \times C_{SIC} \times K \quad (2)$$

where M_{SOC} is the SOC stocks ($Mg\ ha^{-1}$); M_{SIC} is the SIC stocks ($Mg\ ha^{-1}$); D is soil depth (cm); B is the soil bulk density ($g\ cm^{-3}$); C_{SOC} is the SOC content ($g\ kg^{-1}$); C_{SIC} is the SIC content ($g\ kg^{-1}$); K is the proportional coefficient. Specifically, the proportional coefficients for soil at the slope crest, upper slope, middle slope, lower slope, and furrow sole positions are 0.26, 0.26, 0.24, 0.17, and 0.07, respectively, calculated based on the proportion of each part to the whole ditch.

The soil TC stocks at different slope sampling positions are as follows:

$$M_{TC} = M_{SIC} + M_{SOC} \quad (3)$$

where M_{TC} is the TC stocks ($Mg\ ha^{-1}$).

The organic carbon and inorganic carbon stocks of soil in the POM and MAOM fractions are obtained as follows:

$$M_{PSOC} = M_{SOC} \times P \quad (4)$$

$$M_{PSIC} = M_{SIC} \times P \quad (5)$$

$$M_{MSOC} = M_{SOC} \times (1 - P) \quad (6)$$

$$M_{MSIC} = M_{SIC} \times (1 - P) \quad (7)$$

where M_{PSOC} is the organic carbon stocks in the POM fraction ($Mg\ ha^{-1}$); M_{PSIC} is the inorganic carbon stocks in the POM fraction ($Mg\ ha^{-1}$); M_{MSOC} is the organic carbon stocks in the MAOM fraction ($Mg\ ha^{-1}$); M_{MSIC} is the inorganic carbon stocks in the MAOM fraction ($Mg\ ha^{-1}$); and P is the ratio of the POM fraction soil in the bulk soil.

2.5. Data Analysis

After testing the normality (Shapiro–Wilk’s test) and homogeneity of variances (Levene’s test) for all measured variables, the differences in soil properties (TC, SOC, SIC, DOC, SOC_{POM} , SOC_{MAOM} , SIC_{POM} , and SIC_{MAOM} ; TN, NH_4^+ -N, NO_3^- -N, TP, AP, pH, EC, and SWC) among different reclamation years, soil depths, and slope sampling positions were examined using a one–way analysis of variance (ANOVA) with the least significant difference (LSD) test. The differences in soil carbon stocks (M_{TC} , M_{SOC} , M_{SIC} , M_{PSOC} , M_{MSOC} , M_{PSIC} , and M_{MSIC}) were also tested. Additionally, a three–way ANOVA with the least significant difference (LSD) test was used to determine the effects of reclamation years, soil depths, slope sampling locations, and their interactions on the determined soil properties. Linear regression analysis was conducted to determine the overall and grouped relationships (based on reclamation years and soil depth) between organic carbon and inorganic carbon contents in different soil fractions (SOC vs. SIC; SOC_{POM} vs. SIC_{POM} ; and SOC_{MAOM} vs. SIC_{MAOM}). Pearson correlation analysis was performed to assess the relationships between soil carbon contents (TC, SOC, SIC, DOC, SOC_{POM} , SOC_{MAOM} , SIC_{POM} , and SIC_{MAOM}) and soil properties (TN, NH_4^+ -N, NO_3^- -N, TP, AP, pH, EC, and SWC). All results were considered statistically significant at $p < 0.05$ and the statistical analyses were conducted using SPSS (version 22.0.0.0, SPSS, Chicago, IL, USA).

After conducting Detrended Correspondence Analysis (DCA) using Canoco 5 (Version 5.0, Microcomputer Power, Ithaca, NY, USA), Redundancy Analysis (RDA) was performed to further determine the relationship between soil carbon content and other determined soil properties and to calculate the contribution of soil properties to soil carbon content. Structural Equation Modeling (SEM) was constructed using AMOS (Version 28, SPSS, IBM Corp, Armonk, NY, USA) to investigate the direct and indirect effects of reclamation years on SOC_{POM} , SOC_{MAOM} , SIC_{POM} , SIC_{MAOM} , DOC, and SIC in drainage ditch soils. The goodness of fit of the structural equation model was evaluated based on the chi-square

test (χ^2 -text), degrees of freedom (DF), p -value, goodness-of-fit index (GFI), adjusted goodness-of-fit index (AGFI), comparative fit index (CFI), standardized root mean square residual (SRMR), and root mean square error of approximation (RMSEA).

3. Results

3.1. Changes in Physicochemical Properties of Saline–Alkali Ditch Soil after Reclamation

The changes in the soil properties in saline–alkali ditches after reclamation are presented in Table 1. The TC content exhibited a significant decrease from 13.90 to 13.76 g kg⁻¹ with the increasing reclamation years ($p < 0.05$). No significant differences were observed in SOC and SIC contents among different reclamation years ($p > 0.05$). However, the SOC content significantly decreased from 3.30 g kg⁻¹ over 0–20 cm to 2.82 g kg⁻¹ over 40–60 cm ($p > 0.05$), while the DOC content exhibited a significant decrease from about 48 to 36 mg kg⁻¹ with the increasing reclamation years ($p < 0.05$). On the other hand, the SOC_{MAOM} content showed a significant increase from 0.65 to 1.70 g kg⁻¹ with increasing reclamation years ($p < 0.05$), whereas both the SOC_{POM} and SIC_{POM} content experienced significant decreases from 2.24 to 1.12 g kg⁻¹ and from 10.54 to 9.54 g kg⁻¹, respectively ($p < 0.05$). The TN and AP content significantly decreased from 143.07 to 112.60 mg kg⁻¹ and from 26.39 to 20.30 mg kg⁻¹ with increasing reclamation years, respectively ($p < 0.05$), while the NO₃⁻-N content significantly increased from 19.46 to 20.13 mg kg⁻¹ and from 0.48 to 0.55 g kg⁻¹, respectively ($p < 0.05$). Additionally, SWC significantly increased from 26.05 to 29.88% with the increasing reclamation time and from 25.07 to 26.45% with the increasing soil depth ($p < 0.05$). Soil pH showed a significant increase from 8.51 to 9.21 with increasing reclamation years ($p < 0.05$); however, a decrease with no significant differences was found in the NH₄⁺-N content and EC ($p > 0.05$).

Table 1. Soil properties of the saline–alkali ditches under the different reclamation years and soil depths.

	Reclamation Years		
	1st Year	7th Year	15th Year
TC (g kg ⁻¹)	13.90 ± 0.33 ^a	15.03 ± 0.43 ^{ab}	13.76 ± 0.22 ^b
SOC (g kg ⁻¹)	2.89 ± 0.12 ^a	3.52 ± 0.24 ^a	2.94 ± 0.11 ^a
SIC (g kg ⁻¹)	11.01 ± 0.25 ^a	11.51 ± 0.30 ^a	10.83 ± 0.15 ^a
DOC (mg kg ⁻¹)	48.18 ± 3.48 ^a	47.01 ± 2.68 ^{ab}	36.25 ± 2.68 ^b
SOC _{POM} (g kg ⁻¹)	2.24 ± 0.13 ^b	2.99 ± 0.25 ^a	1.23 ± 0.13 ^c
SOC _{MAOM} (g kg ⁻¹)	0.65 ± 0.10 ^b	0.53 ± 0.07 ^b	1.70 ± 0.24 ^a
SIC _{POM} (g kg ⁻¹)	9.86 ± 0.17 ^{ab}	10.54 ± 0.30 ^a	9.55 ± 0.13 ^b
SIC _{MAOM} (g kg ⁻¹)	1.15 ± 0.17 ^a	0.98 ± 0.10 ^a	1.28 ± 0.13 ^a
TN (mg kg ⁻¹)	143.07 ± 13.12 ^b	343.35 ± 24.98 ^a	112.60 ± 11.35 ^b
NH ₄ ⁺ -N (mg kg ⁻¹)	3.71 ± 0.32 ^a	4.00 ± 0.36 ^a	3.34 ± 0.41 ^a
NO ₃ ⁻ -N (mg kg ⁻¹)	19.46 ± 0.13 ^b	20.00 ± 0.12 ^a	20.13 ± 0.09 ^a
TP (g kg ⁻¹)	0.48 ± 0.01 ^b	0.55 ± 0.01 ^a	0.50 ± 0.01 ^b
AP (mg kg ⁻¹)	26.39 ± 1.39 ^a	20.30 ± 1.39 ^b	27.86 ± 1.81 ^{ab}
SWC (%)	26.05 ± 0.52 ^b	21.83 ± 1.04 ^c	29.88 ± 0.63 ^a
pH	8.51 ± 0.03 ^b	8.62 ± 0.03 ^b	9.21 ± 0.03 ^a
EC (μs cm ⁻¹)	3573.88 ± 366.98 ^a	1150.90 ± 72.82 ^a	1030.53 ± 98.89 ^a
	Soil Depths		
	0–20 cm	20–40 cm	40–60 cm
TC (g kg ⁻¹)	14.60 ± 0.34 ^a	13.96 ± 0.30 ^a	14.11 ± 0.40 ^a
SOC (g kg ⁻¹)	3.40 ± 0.155 ^a	3.06 ± 0.19 ^{ab}	2.82 ± 0.15 ^b
SIC (g kg ⁻¹)	11.20 ± 0.24 ^a	10.90 ± 0.20 ^a	11.29 ± 0.29 ^a
DOC (mg kg ⁻¹)	51.43 ± 2.75 ^a	38.14 ± 2.35 ^a	41.38 ± 3.89 ^a
SOC _{POM} (g kg ⁻¹)	2.20 ± 0.19 ^a	2.06 ± 0.22 ^a	2.08 ± 0.16 ^a

Table 1. Cont.

	Soil Depths		
	0–20 cm	20–40 cm	40–60 cm
SOC _{MAOM} (g kg ⁻¹)	1.20 ± 0.19 ^a	1.00 ± 0.20 ^a	0.75 ± 0.12 ^a
SIC _{POM} (g kg ⁻¹)	10.04 ± 0.18 ^a	9.74 ± 0.21 ^a	10.18 ± 0.27 ^a
SIC _{MAOM} (g kg ⁻¹)	1.16 ± 0.16 ^a	1.16 ± 0.13 ^a	1.11 ± 0.11 ^a
TN (mg kg ⁻¹)	216.86 ± 21.11 ^a	193.34 ± 23.97 ^a	187.05 ± 20.87 ^a
NH ₄ ⁺ -N (mg kg ⁻¹)	4.07 ± 0.35 ^a	3.48 ± 0.38 ^a	3.45 ± 0.36 ^a
NO ₃ ⁻ -N (mg kg ⁻¹)	19.76 ± 0.11 ^a	19.90 ± 0.12 ^a	19.94 ± 0.13 ^a
TP (g kg ⁻¹)	0.51 ± 0.01 ^a	0.52 ± 0.01 ^a	0.51 ± 0.01 ^a
AP (mg kg ⁻¹)	25.74 ± 1.33 ^a	24.11 ± 1.53 ^a	24.66 ± 2.02 ^a
SWC (%)	25.07 ± 1.02 ^c	26.35 ± 0.81 ^b	26.45 ± 0.71 ^a
pH	8.76 ± 0.05 ^a	8.79 ± 0.05 ^a	8.80 ± 0.05 ^a
EC (μs cm ⁻¹)	1993.83 ± 321.72 ^a	1993.89 ± 229.98 ^a	1848.88 ± 246.65 ^a

Values are mean ± standard error. Different lowercase letters of the same variable indicate significant differences at the level of $p < 0.05$. (TC, soil total carbon; SOC, soil organic carbon; SIC, soil inorganic carbon; DOC, soil dissolved organic carbon; SOC_{POM}, SOC in POM fraction; SOC_{MAOM}, SOC in MAOM fraction; SIC_{POM}, SIC in POM fraction; SIC_{MAOM}, SIC in MAOM fraction; TN, soil total nitrogen; NH₄⁺-N, soil soluble ammonium nitrogen; NO₃⁻-N, soil soluble nitrate nitrogen; TP, soil total phosphorus; AP, soil available phosphorus; SWC, soil water content; pH, soil pH; and EC, soil electrical conductivity).

The three-way ANOVA conducted on soil properties in saline–alkali ditches (Table 2) revealed that reclamation years had the most significant impact on soil properties. However, the contents of SIC, SIC_{POM}, and NO₃⁻-N did not display any significant responses to changes in reclamation years, soil depth, slope sampling position, or their interactions ($p > 0.05$). Furthermore, soil depth had a significant impact on DOC content and SWC ($p < 0.01$), whereas soil sampling location had a significant impact on the SOC_{MAOM} content and SWC ($p < 0.05$).

Table 2. The results (F values) of three-way ANOVA for soil properties in the saline–alkali ditches.

	R	D	S	R × D	R × S	D × S	R × D × S
TC	3.64 *	0.86	0.44	0.24	0.89	0.43	0.25
SOC	3.38 *	2.85	0.39	0.54	0.66	0.24	0.36
SIC	2.33	1.20	1.16	1.37	0.93	0.71	0.52
DOC	4.38 *	6.42 **	0.89	1.09	1.63	0.48	0.91
SOC _{POM}	16.68 ***	0.50	1.13	0.52	0.96	0.28	0.45
SOC _{MAOM}	30.86 ***	1.08	3.15*	0.21	3.15 **	0.53	1.18
SIC _{POM}	5.82 *	1.39	0.70	1.16	0.97	0.50	0.48
SIC _{MAOM}	1.52	0.02	0.81	0.43	1.28	0.96	0.64
TN	43.09 ***	0.72	0.79	0.70	0.90	0.44	0.48
NH ₄ ⁺ -N	0.66 ***	0.67	0.92	0.40	0.40	0.38	0.48
NO ₃ ⁻ -N	8.10	0.67	1.50	1.08	1.00	0.81	0.59
TP	15.78 ***	0.37	1.44	0.59	1.48	1.35	0.92
AP	6.78 **	0.29	0.85	0.29	1.81	0.42	0.44
SWC	53.29 ***	90.19 ***	14.99 ***	1.58	2.02*	19.54 ***	1.56
pH	199.31 ***	0.95	1.37	1.49	0.85	0.59	0.74
EC	34.82 ***	0.53	1.60	0.76	1.93	0.16	0.21

* $p < 0.05$, ** $p < 0.01$, and *** $p < 0.001$; R, reclamation years; D, depth; S, slope sampling position; TC, soil total carbon; SOC, soil organic carbon; SIC, soil inorganic carbon; DOC, soil dissolved organic carbon; SOC_{POM}, SOC in POM fraction; SOC_{MAOM}, SOC in MAOM fraction; SIC_{POM}, SIC in POM fraction; SIC_{MAOM}, SIC in MAOM fraction; TN, soil total nitrogen; NH₄⁺-N, soil soluble ammonium nitrogen; NO₃⁻-N, soil soluble nitrate nitrogen; TP, soil total phosphorus; AP, soil available phosphorus; SWC, soil water content; pH, soil pH; and EC, soil electrical conductivity.

3.2. Changes in Soil Carbon Stocks in Saline–Alkali Ditches after Reclamation

The soil carbon stocks in saline–alkali drainage ditches varied, as shown in Figure 2. M_{TC}, M_{SOC}, and M_{SIC} (Figure 2a–c), along with M_{PSIC} and M_{MSIC} (Figure 2f,g), did not show any significant differences across different reclamation years ($p > 0.05$). However,

M_{PSOC} significantly decreased from 19.02 to 12.71 $Mg\ ha^{-1}$, while M_{MSOC} significantly increased from 5.30 to 12.27 $Mg\ ha^{-1}$ in the 15th year compared to the 1st year ($p < 0.05$). Furthermore, among the different soil sampling positions in the saline-alkali ditches, M_{MSOC} exhibited no significant differences, while M_{PSIC} showed no significant differences except in the 15th year ($p > 0.05$). Notably, the soil carbon stocks of other components varied significantly among the lower slope, furrow sole, and other soil sampling positions. Generally, the carbon stocks in the lower slope and furrow sole positions were significantly lower than those in the other soil sampling positions ($p < 0.05$).

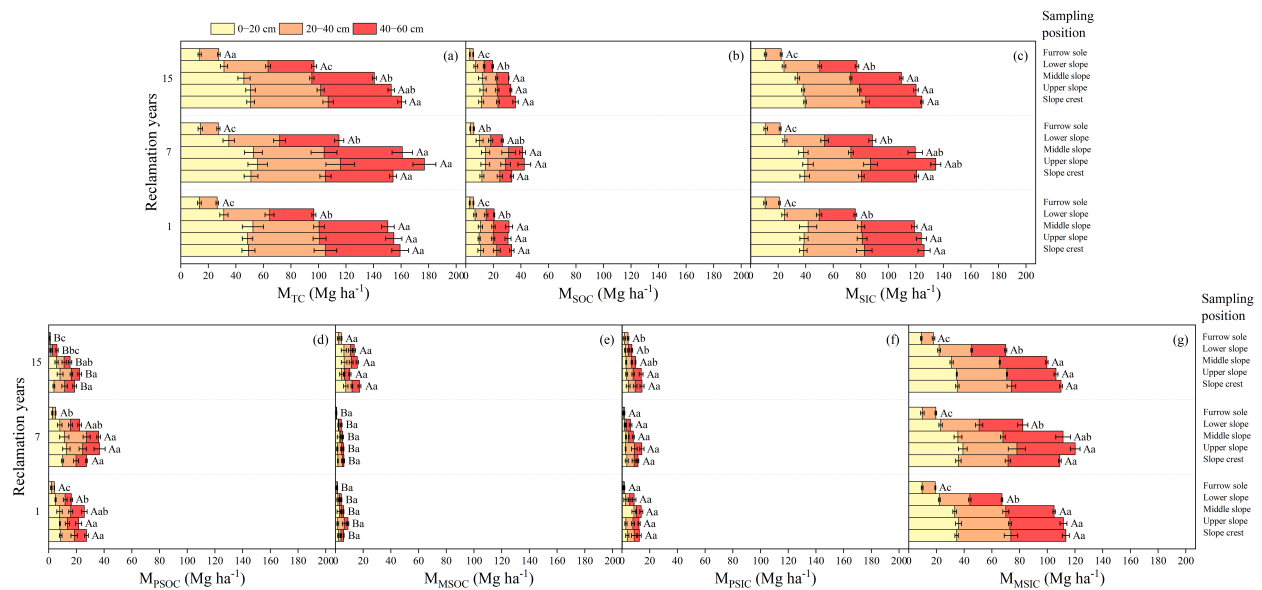


Figure 2. Effect of different reclamation years and slope sampling positions on (a) M_{TC} , (b) M_{SOC} , (c) M_{SIC} , (d) M_{PSOC} , (e) M_{MSOC} , (f) M_{PSIC} , and (g) M_{MSIC} at average level per 20 cm in 0–60 cm soil depth. Different lowercase letters denote significant differences among different slope sampling positions in the same reclamation year ($p < 0.05$); different uppercase letters denote significant differences among different reclamation years ($p < 0.05$). (M_{TC} , TC stock; M_{SOC} , SOC stock; M_{SIC} , SIC stock; M_{PSOC} , SOC_{POM} stock; M_{MSOC} , SOC_{MAOM} stock; M_{PSIC} , SIC_{POM} stock; and M_{MSIC} , SIC_{MAOM} stock).

3.3. Correlation between Different Components of SOC and SIC

The linear regression analysis results (Figure 3) demonstrated the positive correlation between SOC and SIC overall (Figure 3a; $R^2 = 0.33$), as well as between SOC_{MAOM} and SIC_{MAOM} (Figure 3b; $R^2 = 0.21$), and between SOC_{POM} and SIC_{POM} (Figure 3d; $R^2 = 0.18$, $p < 0.05$). Only the relationship between SOC_{POM} and SIC_{POM} in the 15th year showed a significant negative correlation (Figure 3e; $R^2 = 0.04$, $p < 0.05$) among the different reclamation year groups. The correlations between the organic carbon and inorganic carbon contents of other components were significantly positive (Figure 3d–f; $p < 0.05$). Similarly, a significant positive correlation between the organic carbon and inorganic carbon contents was found in each component among the different soil depth groups (Figure 3g–i; $p < 0.05$).

3.4. Direct and Indirect Effects of Reclamation Time on Different Soil Carbon Components

The SEM results showed that the reclamation years indirectly promoted the increase in SIC content by promoting the increase in SOC_{MAOM} content, thereby indirectly increasing SIC_{MAOM} content (Figure 4). The reclamation years and SOC_{POM} content promoted SIC content by suppressing the increase in SIC_{POM} and SIC_{MAOM} contents. The reclamation years inhibited SOC_{MAOM} and SIC_{MAOM} contents by suppressing DOC content. Additionally, DOC content indirectly increased SIC content by promoting SOC_{MAOM} and SIC_{MAOM} contents.

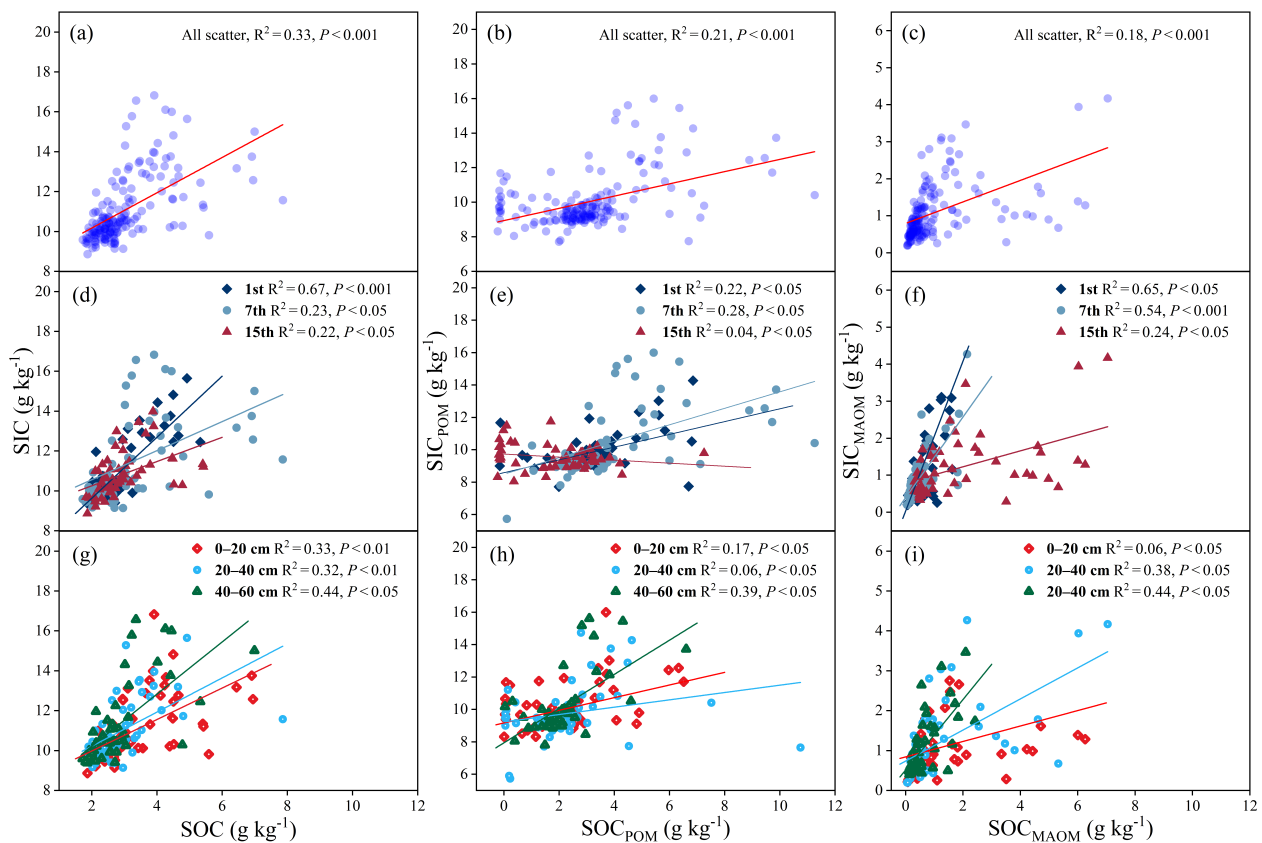
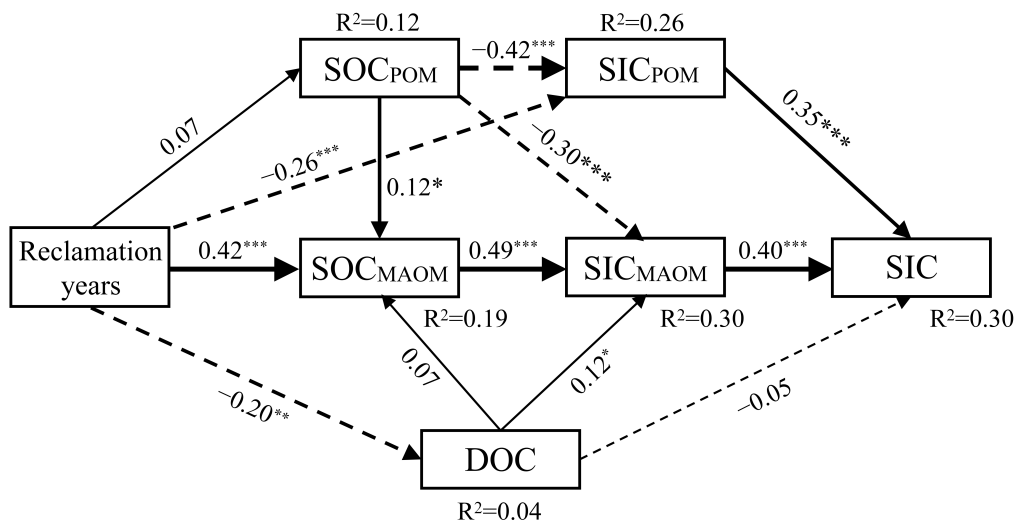


Figure 3. Relationship between SOC and SIC (a,d,g), SOC_{POM} and SIC_{POM} (b,e,h), and SOC_{MAOM} and SIC_{MAOM} (c,f,i) under the grouping of reclamation years and depth. All fitting curves are at the significance level of $p < 0.05$. (SOC, soil organic carbon; SIC, soil inorganic carbon; SOC_{POM}, SOC in POM fraction; SOC_{MAOM}, SOC in MAOM fraction; SIC_{POM}, SIC in POM fraction; and SIC_{MAOM}, SIC in MAOM fraction).



$\chi^2 = 1.83$, DF = 8, $P = 0.05$ n = 168, GFI = 0.98, AGFI = 0.92, CFI = 0.97, SRMR = 0.04, RMSEA = 0.04

Figure 4. Direct and indirect effects of the reclamation years on SOC_{POM}, SOC_{MAOM}, SIC_{POM}, SIC_{MAOM}, DOC, and SIC in the saline-alkali ditches. The solid arrows represent a positive relationship

and the dashed arrows represent a negative relationship, respectively. The width of the arrow is proportional to the strength of the relationship, and the adjacent numbers on arrows represent standardized path coefficients. R^2 represents the proportion of variance explained by the model. * $p < 0.05$, ** $p < 0.01$, and *** $p < 0.001$. (SIC, soil inorganic carbon; DOC, soil dissolved organic carbon; SOC_{POM}, SOC in POM fraction; SOC_{MAOM}, SOC in MAOM fraction; SIC_{POM}, SIC in POM fraction; and SIC_{MAOM}, SIC in MAOM fraction).

3.5. The Primary Factors Affecting the Soil Carbon Content of Different Components

The results of the Pearson correlation analysis showed that TN, AP, SWC, pH, and EC were the primary factors influencing the measured soil carbon content (Figure 5). Moreover, the RDA results demonstrated that the first two axes accounted for 21.74% and 7.31% of the variation in soil carbon content, respectively (Figure S1). These findings suggest that these soil physicochemical parameters collectively explained 33.10% of the total variation (Table S2). Additionally, the contribution of each soil physicochemical parameter in explaining the changes in soil carbon content of different components were ranked as follows: TN > AP > EC > SWC > pH (Table 3).

Based on a comprehensive analysis of the Pearson correlation and RDA results (Figures 5 and S1), several significant positive correlations were observed between TN and the TC, SOC, SIC, and SIC_{POM} contents ($p < 0.05$). These significant positive correlations were found between AP and the SOC, SIC, SOC_{MAOM}, and SIC_{MAOM} contents ($p < 0.05$). Conversely, pH exhibited significant negative correlations with TC, SOC, and SIC_{POM} contents ($p < 0.05$), while SWC showed significant negative correlations with SOC and DOC contents ($p < 0.05$). Notably, SWC and pH demonstrated significant positive correlations with SOC_{MAOM} content ($p < 0.05$), whereas EC exhibited a significant negative correlation with the SOC_{MAOM} and SIC_{MAOM} contents ($p < 0.05$).

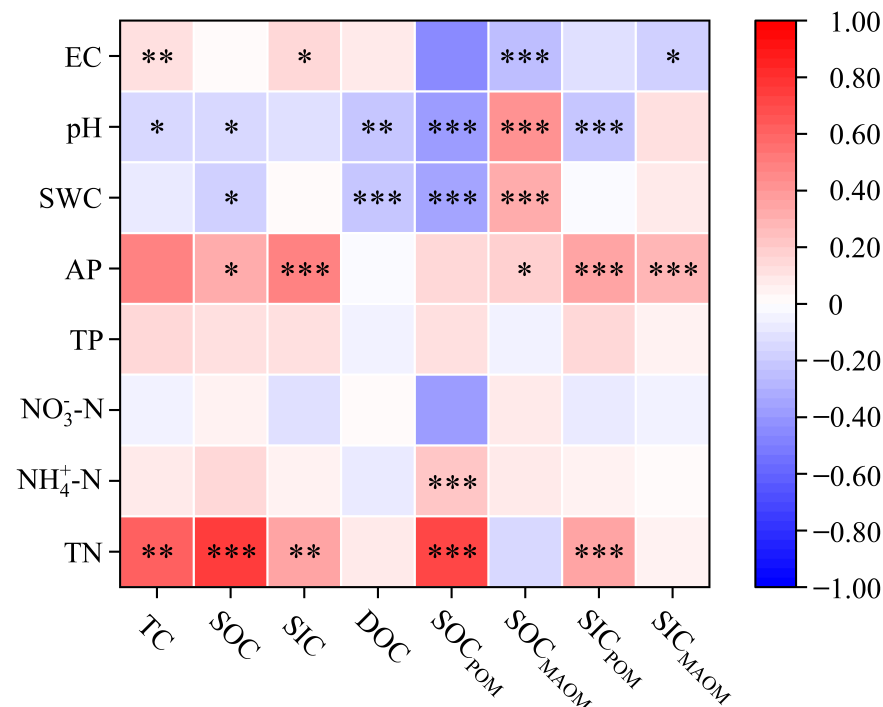


Figure 5. Pearson's correlations between soil carbon contents and soil physicochemical properties. (* $p < 0.05$, ** $p < 0.01$, and *** $p < 0.001$; TC, soil total carbon; SOC, soil organic carbon; SIC, soil inorganic carbon; DOC, soil dissolved organic carbon; SOC_{POM}, SOC in POM fraction; SOC_{MAOM}, SOC in MAOM fraction; SIC_{POM}, SIC in POM fraction; SIC_{MAOM}, SIC in MAOM fraction; TN, soil total nitrogen; NH₄⁺-N, soil soluble ammonium nitrogen; NO₃⁻-N, soil soluble nitrate nitrogen; TP, soil total phosphorus; AP, soil available phosphorus; SWC, soil water content; pH, soil pH; and EC, soil electrical conductivity.)

Table 3. Importance and significance test of soil properties' contribution rankings.

Rankings	Environment Factors	Contribution/%	Pseudo-F	<i>p</i>
1	TN	48.50	31.80	0.002
2	AP	21.50	15.30	0.002
3	EC	14.70	11.10	0.002
4	SWC	5.20	4.00	0.002
5	pH	4.30	3.30	0.004
6	NH ₄ ⁺ -N	4.10	3.20	0.008
7	NO ₃ ⁻ -N	1.10	0.90	0.47
8	TP	0.70	0.60	0.68

TN, soil total nitrogen; NH₄⁺-N, soil soluble ammonium nitrogen; NO₃⁻-N, soil soluble nitrate nitrogen; TP, soil total phosphorus; AP, soil available phosphorus; SWC, soil water content; pH, soil pH; and EC, soil electrical conductivity.

4. Discussion

4.1. Dynamics of the Soil Carbon Pool in Saline–alkali Ditches after Reclamation

The results demonstrate that the increasing reclamation time did not have a significant impact on the SOC and SIC contents of the saline–alkali ditches (Table 1; Figure 2b,c). This unchanging trend in SOC and SIC contents with respect to reclamation time differs from previous research on reclaimed saline–alkali farmland [11,47,48]. In farmland, SOC tends to increase due to fertilization and the accumulation of organic residues, while SIC decreases because of irrigation and precipitation [11]. The reasons for these discrepant results are attributed to two main factors. Firstly, reclaimed saline–alkali ditches are subject to less influence from agricultural activities compared to farmland, which allows for a greater input of carbon from plants into the soil; however, this input is still limited in comparison to the effects of fertilization and the presence of organic residues. Secondly, the structure of the ditches leads to higher groundwater levels and moisture content compared to farmland, potentially inhibiting the microbial mineralization of soil carbon [49].

Additionally, the reclamation years did not affect the storage capacity of the soil carbon pool but influenced the compositions therein (Figure 2). These results indicate a unique carbon fixation process in coastal saline–alkali ditches. Specifically, the findings demonstrate that as the reclamation time increased, a notable decrease was found in the levels of SOC_{POM} and SIC_{POM} contents, while SOC_{MAOM} content increased (Table 1). Similarly, the M_{PSOC} showed a decreasing trend, whereas the M_{MSOC} increased (Figure 2d,e). This result indicates that the changes in different soil carbon components are inherent factors for maintaining constant soil carbon stock, and it may be due to a conversion from SOC_{POM} to SOC_{MAOM} during the reclamation. In addition, the significant decrease in SOC_{POM} and increase in SOC_{MAOM} at the furrow sole position indicate greater stability of soil carbon in this position. This is because POM has a shorter residence time and faster decomposition rate in the soil compared to MAOM [50–52].

The reclamation years have a significant impact on the different fractions of soil carbon pools in saline–alkali ditches (Table 2). In addition, the response of different soil carbon components to the reclamation years, constituting an inherent factor, affect the changes in soil carbon pool (Table S2; Figure 4). In light of the correlation between SOC and SIC contents in the soil fractions of POM and MAOM and the SEM results driven by the reclamation years (Figures 3 and 4), the process of changes in soil carbon components of saline–alkali ditches after reclamation may be as follows (Figure 6). Firstly, after the reclamation, the saline–alkali soil conditions gradually improve with an increase in reclamation time (Table 1). This improvement leads to the colonization and growth of numerous plants (Table S1), resulting in the entrance of plant residues into the soil. These organic materials further decompose into SOC_{POM}, SOC_{MAOM}, and DOC through microbial metabolisms. Secondly, due to the different turnover rates of POM and MAOM, SOC_{POM} rapidly accumulates between the 1st and 7th year (Table 1), meanwhile, it gradually recomposes into SIC_{POM} and SOC_{MAOM} through continuous biotic and abiotic processes.

Thirdly, between the 7th and 15th year, SOC_{POM} contents/stocks decrease due to the continuous microbial transformation and consumption (Figure 1). Some of the carbon therein is converted into SOC_{MAOM} (Table 1; Figure 3c,f,i) and is decomposed to CO_2 and/or carbonates, which may accelerate the formation of insoluble compounds, e.g., the SIC_{POM} (Figures 3e and 4). Fourthly, SOC_{MAOM} significantly increases with reclamation due to the inputs of plant residues and the transformation of SOC_{POM} (Figure 4). The formation of SIC_{MAOM} predominantly occurs through the transformation of SOC_{MAOM} and DOC (Figure 4). These results together suggest that the stability of the soil carbon pool has been changed after the reclamation.

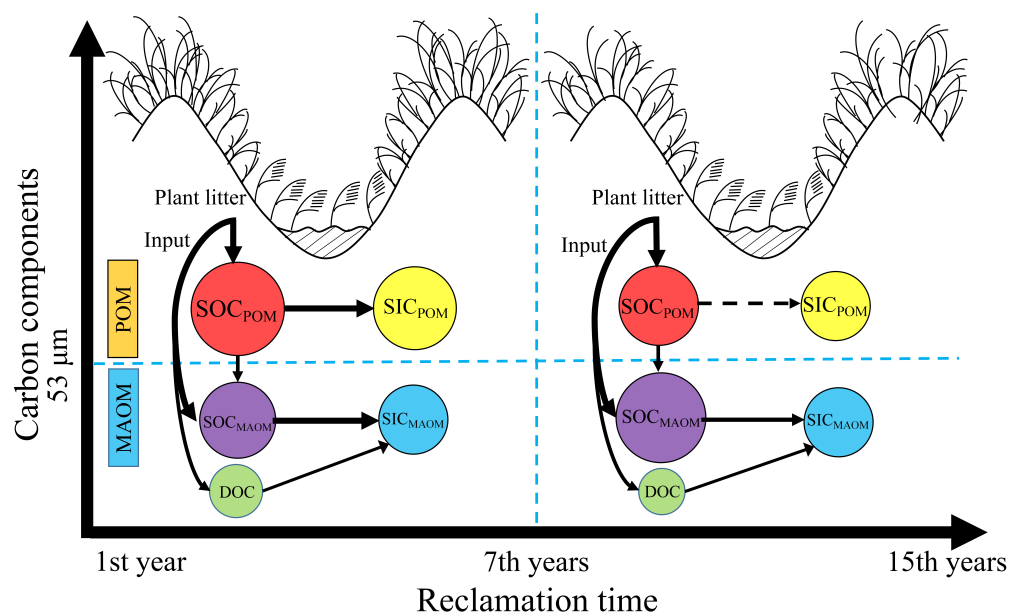


Figure 6. Conceptual framework for the conversion of soil organic carbon and inorganic carbon based on reclamation time and soil carbon components. The solid arrows represent a conversion relationship, and the dashed arrow represents no conversion relationship. The width of the arrow is proportional to the strength of the conversion relationship. (SIC, soil inorganic carbon; DOC, soil dissolved organic carbon; SOC_{POM} , SOC in POM fraction; SOC_{MAOM} , SOC in MAOM fraction; SIC_{POM} , SIC in POM fraction; SIC_{MAOM} , SIC in MAOM fraction.).

With an increase in reclamation years of saline–alkali ditches, the stability of the soil carbon pool improves (Table 1; Figure 2). This stability is largely influenced by the proportion of stable carbon in the pool. Previous studies have shown that the stability of POM primarily occurs via the encapsulation or formation of microaggregates (53–250 μm) and the stabilization of microbial residues on silt and clay (<53 μm) surfaces [27,52,53]. Therefore, the increase in MAOM contributes to the stability of the soil carbon pool, which is consistent with our own findings (Table 1; Figure 2d,e). Additionally, the SOC_{POM} exhibited a negative correlation with the SIC_{POM} in the 15th year, in contrast to other reclamation times. This suggests that the POM decreased as the reclamation time increased, leading to an improvement in the stability of the soil carbon pool. Although DOC is the main and more effective pathway for the formation of SOC_{MAOM} [16,33], a significant decrease in DOC with reclamation years also indicates an improvement in the stability of the soil carbon pool (Table 1). However, the SEM results demonstrate that DOC has a promoting effect on the formation of SOC_{MAOM} with no significance ($p > 0.05$), while it significantly promotes the formation of SIC_{MAOM} (Figure 4). This could be attributed to changes in plant biomass and an increase in soil pH resulting from reclamation activities (Tables 1 and S1).

In recent years, several models have been proposed regarding the formation mechanisms of POM and MAOM [54,55]. In these models, POM is expected to form from partially decomposed plant residues once they enter the soil. As a result, it is believed that POM

does not transform as MAOM after decomposition [16,56]. However, other studies suggest that during the process of POM decomposition, lower molecular weight soluble organic compounds are formed, such as DOC [33]. Additionally, POM is mineralized by microbial metabolisms or bound to minerals to form MAOM [57,58]. These different perceptions highlight the complexity of the POM to MAOM transformation process and suggest that it may not solely depend on the conversion of soluble organic compounds. Though the application of isotopic and chemical analysis is still necessary to confirm our research findings, our results indicate a possible transformation from SOC_{POM} to SOC_{MAOM} between POM and MAOM. Nonetheless, this suggests that in soil environments where DOC is easily removed, such as in frequently drained ditch environments, the transformation from POM to MAOM may be more likely to occur. Our results further indicate a unique carbon fixation process in coastal saline–alkali ditches, that is, although the storage has not increased following the reclamation years, the stability has increased.

4.2. The Primary Factors Affecting Soil Carbon Pools in Saline–alkali Ditches

For the saline–alkali ditches, TN and AP were identified as the predominant factors contributing to promoting the increase in different soil carbon components (Table 3; Figures 5 and Figure S1). This is mainly attributed to the fact that nitrogen and phosphorus are essential elements for plant growth [59]; plant growth may facilitate the increase in the soil carbon pool. However, no increase in soil carbon stocks in saline–alkali ditch is likely due to the opposite variations in TN and AP contents following reclamation (Table 1). In the early stage of saline–alkali farmland development, a large amount of fertilizer will be applied to improve soil nutrients. In view of the different migration processes of the elements of N and P, irrigation and salt drainage process can lead to the migration of N to the ditch, resulting in the phenomenon of total nitrogen increasing first and then decreasing following reclamation of the ditch [60].

Although EC, SWC, and pH inhibited the increase in different soil carbon components, their combined effect increased the soil carbon pool stability (Tables 1 and 3; Figures 5 and S1). Our results showed no significant decrease in EC, whereas significant decreases in pH and SWC were shown (Table 1). Moreover, the significant negative correlation between EC and SOC_{MAOM} , and the significant positive correlation between SWC, pH, and SOC_{MAOM} , suggest that EC, SWC, and pH all contribute to the accumulation of SOC_{MAOM} (Figures 5 and S1). The changes in EC, SWC, and pH possibly inhibit microbial activity, making SOC_{MAOM} easier to accumulate, which contributes to increasing the soil carbon pool stability. Additionally, SWC and pH were significantly negatively correlated with SOC and DOC contents, indicating that the increase in SWC and pH after reclamation inhibited the production of SOC and DOC (Table 1; Figures 5 and S1). It should be noted that the mechanisms behind these inhibitory effects are not the same. This is because excessive SWC creates water stress, which reduces plant net primary productivity and even leads to plant death [61–63]. This, in turn, results in a reduction in the input of soil carbon. On the other hand, a higher soil pH ($pH > 8$) may increase the desorption and release of SOC and DOC from the soil, ultimately leading to a decrease in SOC and DOC contents [21,64].

In summary, our research results suggest that the main factors affecting the soil carbon pool in reclaimed saline–alkali ditches are TN, AP, EC, SWC, and pH. An increase in TN and AP contents raises carbon contents, while an increase in EC, SWC, and pH reduces carbon contents. However, the combined changes in these factors result in the overall stability of the soil carbon pool, with variations observed between POM and MAOM fractions in saline–alkali ditches. Although the continuous accumulation of SOC_{MAOM} indicates an ongoing increase in soil carbon pool stability during reclamation (Figure 2), the build-up of SOC_{MAOM} in the short-term reclamation process is still insufficient compared to the entire soil carbon pool. It requires the maintenance of high biomass in the saline–alkali ditches to increase the soil MAOM fraction. Compared to the saline–alkali farmland, saline–alkali ditches are hardly directly affected by agricultural activities after reclamation.

These activities include physical soil disturbance caused by agricultural machinery and the application of fertilizers and pesticides, as well as irrigation and drainage. Instead, they are indirectly impacted, which causes the saline–alkali ditch soil carbon pool to be controlled by farmland management measures to some extent. Therefore, we suggest emptying as much water as possible from the drainage ditches following irrigation in the adjacent saline–alkali farmland. The drainage process would reduce the negative effects caused by the waterlogging and salinity in the ditches, which could accelerate soil nutrient utilization, promote plant biomass growth and microbial activities, and may increase the carbon stock of the saline–alkali ditches.

Although our data have shown the potential transformation of SOC_{POM} to SOC_{MAOM} in the soil carbon pool, more direct evidence is still required to confirm this process. To gain a more comprehensive and specific understanding of this process, it is necessary to utilize techniques such as isotopic and infrared spectroscopy, as well as different mathematical models to simulate soil carbon dynamics. In addition, to fully evaluate the soil carbon stocks in the saline–alkali ditches, more sufficient data relating to the entire soil profiles, equivalent soil masses, soil bulk density, and a sufficient number of samples are needed in the following studies [65,66]. In conclusion, our results have enriched the academic understanding of the formation and transformation mechanisms of POM and MAOM. Our results further indicate a unique carbon fixation process in coastal saline–alkali ditches, that is, although the storage has not increased following the reclamation years, the stability has increased (Figure 2). As far as we know, the present study firstly provides a case study contributing to a comprehensive and reasonable evaluation of the impact of reclamation of saline–alkali farmland on the soil carbon pool, providing a theoretical basis for the management of the soil carbon pool in the reclaimed saline–alkali areas.

5. Conclusions

In this study, we investigated the dynamics of soil carbon pools in the saline–alkali ditches of the Yellow River Delta using the spatio–temporal substitution method. We also explored the changes in soil carbon components (POM and MAOM) and their stocks in drainage ditches of the reclaimed saline–alkali farmland. In the POM fraction, the SOC_{POM} content and M_{PSOC} significantly decreased from 2.24 to 1.12 g kg^{−1} and from 19.02 to 12.71 Mg ha^{−1}, respectively. Conversely, in the MAOM fraction, the SOC_{MAOM} content and M_{MSOC} significantly increased from 0.65 to 1.70 g kg^{−1} and from 5.30 to 12.27 Mg ha^{−1}, respectively. These results collectively indicate that the potential transformation of SOC_{POM} to SOC_{MAOM} and the mineralization process of SOC_{POM} and SOC_{MAOM} to SIC were the inherent processes that maintain the constant carbon stock of saline–alkali ditch soils. The changes in TN, AP, EC, SWC, and pH over the reclamation time were external factors. Notably, the accumulation of SOC_{MAOM} after reclamation could enhance the stability of the saline–alkali ditch’s soil carbon pool. The results undoubtedly demonstrate that although the storage has not increased following the reclamation years, the stability has increased. As far as we know, the present study firstly provides a case study contributing to a comprehensive and reasonable evaluation of the impact of reclamation of saline–alkali farmland on the soil carbon pool, providing a theoretical foundation for managing the soil carbon pool in recovered saline–alkali areas.

Supplementary Materials: The following supporting information can be downloaded at: <https://www.mdpi.com/article/10.3390/agronomy13112843/s1>, Table S1: Summary of plant height, fresh weight, and coverage under different reclamation years. Table S2: Redundancy analysis results for the soil carbon content of different components. Figure S1: The relative abundance for single factors influences the soil carbon content of different components.

Author Contributions: Writing—review and editing, X.L. and Z.L.; methodology, X.L., Z.L., J.L., H.G. and Y.Z.; validation, J.L., H.G., Y.Z., Z.S. and Z.O.; data curation, X.L., Z.L. and J.L.; conceptualization, Z.S. and Z.O.; project administration, Z.L. All authors have read and agreed to the published version of the manuscript.

Funding: This work was funded by the Strategic Priority Research Program of the Chinese Academy of Sciences (no. XDA26050202), the Shandong Provincial Natural Science Foundation (no. ZR2021QC055), the National Natural Science Foundation of China (no. 32101392), and the Natural Science Foundation of Shandong Province, China (no. ZR2022QC098).

Data Availability Statement: The data presented in this study are available on request from the corresponding author. The data are not publicly available due to privacy restrictions.

Conflicts of Interest: The authors declare no conflict of interest.

References

- Lal, R.; Monger, C.; Nave, L.; Smith, P. The role of soil in regulation of climate. *Philos. Trans. R. Soc. B Biol. Sci.* **2021**, *376*, 20210084. [[CrossRef](#)]
- Wang, S.; Lu, W.; Zhang, F. Vertical distribution and controlling factors of soil inorganic carbon in poplar plantations of coastal eastern China. *Forests* **2022**, *13*, 83. [[CrossRef](#)]
- Lal, R. Soil carbon sequestration impacts on global climate change and food security. *Science* **2004**, *304*, 1623–1627. [[CrossRef](#)]
- Tian, Y.; Wang, Q.; Gao, W.; Luo, Y.; Wu, L.; Rui, Y.; Huang, Y.; Xiao, Q.; Li, X.; Zhang, W. Organic amendments facilitate soil carbon sequestration via organic carbon accumulation and mitigation of inorganic carbon loss. *Land Degrad. Dev.* **2022**, *33*, 1423–1433. [[CrossRef](#)]
- Liu, J.E.; Deng, D.; Zou, C.; Han, R.; Xin, Y.; Shu, Z.; Zhang, L.M. *Spartina alterniflora* saltmarsh soil organic carbon properties and sources in coastal wetlands. *J. Soils Sediments* **2021**, *21*, 3342–3351. [[CrossRef](#)]
- Zamanian, K.; Pustovoytov, K.; Kuzyakov, Y. Pedogenic carbonates: Forms and formation processes. *Earth Sci. Rev.* **2016**, *157*, 1–17. [[CrossRef](#)]
- Zhang, J.H.; Wang, Y.; Li, F.C. Soil organic carbon and nitrogen losses due to soil erosion and cropping in a sloping terrace landscape. *Soil Res.* **2015**, *53*, 87–96. [[CrossRef](#)]
- Kormanek, M.; Banach, J.; Sowa, P. Effect of soil bulk density on forest tree seedlings. *Int. Agrophys.* **2015**, *29*, 67–74. [[CrossRef](#)]
- Wang, C.; Li, L.; Yan, Y.; Cai, Y.; Xu, D.; Wang, X.; Chen, J.; Xin, X. Effects of cultivation and agricultural abandonment on soil carbon, nitrogen and phosphorus in a meadow steppe in Eastern Inner Mongolia. *Agric. Ecosyst. Environ.* **2021**, *309*, 107284. [[CrossRef](#)]
- Cheng, Z.; Zhang, F.; Gale, W.J.; Wang, W.; Sang, W.; Yang, H. Effects of reclamation years on composition and diversity of soil bacterial communities in Northwest China. *Can. J. Microbiol.* **2018**, *64*, 28–40. [[CrossRef](#)]
- Zhang, H.; Yin, A.; Yang, X.; Wu, P.; Fan, M.; Wu, J.; Zhang, M.; Gao, C. Changes in Surface soil organic/inorganic carbon concentrations and their driving forces in reclaimed coastal tidal flats. *Geoderma* **2019**, *352*, 150–159. [[CrossRef](#)]
- Zhang, T.; Song, B.; Han, G.; Zhao, H.; Hu, Q.; Zhao, Y.; Liu, H. Effects of coastal wetland reclamation on soil organic carbon, total nitrogen, and total phosphorus in China: A Meta-analysis. *Land Degrad. Dev.* **2023**, *34*, 3340–3349. [[CrossRef](#)]
- Cui, J.; Liu, C.; Li, Z.; Wang, L.; Chen, X.; Ye, Z.; Fang, C. Long-term changes in topsoil chemical properties under centuries of cultivation after reclamation of coastal wetlands in the Yangtze Estuary, China. *Soil Tillage Res.* **2012**, *123*, 50–60. [[CrossRef](#)]
- Su, Y.; Wang, X.; Yang, R.; Lee, J. Effects of sandy desertified land rehabilitation on soil carbon sequestration and aggregation in an arid region in China. *J. Environ. Manag.* **2010**, *91*, 2109–2116. [[CrossRef](#)]
- Wang, Y.; Jiang, J.; Niu, Z.; Li, Y.; Li, C.; Feng, W. Responses of soil organic and inorganic carbon vary at different soil depths after long-term agricultural cultivation in Northwest China. *Land Degrad. Dev.* **2019**, *30*, 1229–1242. [[CrossRef](#)]
- Cotrufo, M.F.; Soong, J.L.; Horton, A.J.; Campbell, E.E.; Haddix, M.L.; Wall, D.H.; Parton, W.J. Formation of soil organic matter via biochemical and physical pathways of litter mass loss. *Nat. Geosci.* **2015**, *8*, 776–779. [[CrossRef](#)]
- Lange, M.; Eisenhauer, N.; Sierra, C.A.; Bessler, H.; Engels, C.; Griffiths, R.I.; Malik, A.A.; Roy, J.; Scheu, S.; Steinbeiss, S.; et al. Plant diversity increases soil microbial activity and soil carbon storage. *Nat. Commun.* **2015**, *6*, 6707. [[CrossRef](#)] [[PubMed](#)]
- Prommer, J.; Walker, T.W.N.; Wanek, W.; Braun, J.; Zezula, D.; Hu, Y.; Hofhansl, F.; Richter, A. Increased microbial growth, biomass, and turnover drive soil organic carbon accumulation at higher plant diversity. *Glob. Change Biol.* **2020**, *26*, 669–681. [[CrossRef](#)]
- Fan, X.; Pedroli, B.; Liu, G.; Liu, Q.; Liu, H.; Shu, L. Soil salinity development in the Yellow River Delta in relation to groundwater dynamics. *Land Degrad. Dev.* **2012**, *23*, 175–189. [[CrossRef](#)]
- Davidson, E.A.; Janssens, I.A. Temperature sensitivity of soil carbon decomposition and feedbacks to climate change. *Nature* **2006**, *440*, 165–173. [[CrossRef](#)]
- Zhang, K.; Wang, X.; Wu, L.; Lu, T.; Guo, Y.; Ding, X. Impacts of salinity on the stability of soil organic carbon in the croplands of the Yellow River Delta. *Land Degrad. Dev.* **2021**, *32*, 1873–1882. [[CrossRef](#)]
- Cerli, C.; Celi, L.; Kalbitz, K.; Guggenberger, G.; Kaiser, K. Separation of light and heavy organic matter fractions in soil—Testing for proper density cut-off and dispersion level. *Geoderma* **2012**, *170*, 403–416. [[CrossRef](#)]
- Doetterl, S.; Stevens, A.; Six, J.; Merckx, R.; Van Oost, K.; Casanova Pinto, M.; Casanova-Katny, A.; Muñoz, C.; Boudin, M.; Zagal Venegas, E.; et al. Soil carbon storage controlled by interactions between geochemistry and climate. *Nat. Geosci.* **2015**, *8*, 780–783. [[CrossRef](#)]

24. Yu, W.; Huang, W.; Weintraub-Leff, S.R.; Hall, S.J. Where and why do particulate organic matter (POM) and mineral-associated organic matter (MAOM) differ among diverse soils? *Soil Biol. Biochem.* **2022**, *172*, 108756. [[CrossRef](#)]
25. Cambardella, C.A.; Elliott, E.T. Particulate soil organic-matter changes across a grassland cultivation sequence. *Soil Sci. Soc. Am. J.* **1992**, *56*, 777–783. [[CrossRef](#)]
26. Bradford, M.A.; Fierer, N.; Reynolds, J.F. Soil carbon stocks in experimental mesocosms are dependent on the rate of labile carbon, nitrogen and phosphorus inputs to soils. *Funct. Ecol.* **2008**, *22*, 964–974. [[CrossRef](#)]
27. King, A.E.; Congreves, K.A.; Deen, B.; Dunfield, K.E.; Voroney, R.P.; Wagner-Riddle, C. Quantifying the relationships between soil fraction mass, fraction carbon, and total soil carbon to assess mechanisms of physical protection. *Soil Biol. Biochem.* **2019**, *135*, 95–107. [[CrossRef](#)]
28. Rui, Y.; Jackson, R.D.; Cotrufo, M.F.; Sanford, G.R.; Spiesman, B.J.; Deiss, L.; Culman, S.W.; Liang, C.; Ruark, M.D. Persistent soil carbon enhanced in mollisols by well-managed grasslands but not annual grain or dairy forage cropping systems. *Proc. Natl. Acad. Sci. USA* **2022**, *119*, e2118931119. [[CrossRef](#)]
29. Baldock, J.A.; Skjemstad, J.O. Role of the soil matrix and minerals in protecting natural organic materials against biological attack. *Org. Geochem.* **2000**, *31*, 697–710. [[CrossRef](#)]
30. Von Lützow, M.; Kögel-Knabner, I.; Ekschmitt, K.; Flessa, H.; Guggenberger, G.; Matzner, E.; Marschner, B. SOM fractionation methods: Relevance to functional pools and to stabilization mechanisms. *Soil Biol. Biochem.* **2007**, *39*, 2183–2207. [[CrossRef](#)]
31. Kleber, M.; Nico, P.S.; Plante, A.; Filley, T.; Kramer, M.; Swanston, C.; Sollins, P. Old and stable soil organic matter is not necessarily chemically recalcitrant: Implications for modeling concepts and temperature sensitivity. *Glob. Change Biol.* **2011**, *17*, 1097–1107. [[CrossRef](#)]
32. Kallenbach, C.; Frey, S.; Grandy, A. Direct evidence for microbial-derived soil organic matter formation and its ecophysiological controls. *Nat. Commun.* **2016**, *7*, 13630. [[CrossRef](#)] [[PubMed](#)]
33. Sokol, N.W.; Sanderman, J.; Bradford, M.A. Pathways of mineral-associated soil organic matter formation: Integrating the role of plant carbon source, chemistry, and point of entry. *Glob. Change Biol.* **2019**, *25*, 12–24. [[CrossRef](#)] [[PubMed](#)]
34. Haddix, M.L.; Gregorich, E.G.; Helgason, B.L.; Janzen, H.; Ellert, B.H.; Cotrufo, M.F.; Resource, N.; St, W.L.; Collins, F. Climate, carbon content, and soil texture control the independent formation and persistence of particulate and mineral-associated organic matter in soil. *Geoderma* **2020**, *363*, 114160. [[CrossRef](#)]
35. Cotrufo, M.F.; Haddix, M.L.; Kroeger, M.E.; Stewart, C.E. The role of plant input physical-chemical properties, and microbial and soil chemical diversity on the formation of particulate and mineral-associated organic matter. *Soil Biol. Biochem.* **2022**, *168*, 108648. [[CrossRef](#)]
36. Wang, Z.; Zhao, G.; Gao, M.; Chang, C. Spatial variability of soil salinity in coastal saline soil at different scales in the Yellow River Delta, China. *Environ. Monit. Assess.* **2017**, *189*, 80. [[CrossRef](#)]
37. Jia, Z.; Luo, W.; Xie, J.; Pan, Y.; Chen, Y.; Tang, S.; Liu, W. Salinity dynamics of wetland ditches receiving drainage from irrigated agricultural land in arid and semi-arid regions. *Agric. Water Manag.* **2011**, *100*, 9–17. [[CrossRef](#)]
38. Amendola, D.; Mutema, M.; Rosolen, V.; Chaplot, V. Geoderma Soil Hydromorphy and Soil Carbon: A Global Data Analysis. *Geoderma* **2018**, *324*, 9–17. [[CrossRef](#)]
39. Freeman, C.; Fenner, N.; Ostler, N.J.; Kang, H.; Dowrick, D.J.; Reynolds, B.; Lock, M.A.; Sleep, D.; Hughes, S.; Hudson, J. Export of dissolved organic carbon from peatlands under elevated carbon dioxide levels. *Nature* **2004**, *30*, 195–198. [[CrossRef](#)]
40. Yan, N.; Marschner, P.; Cao, W.; Zuo, C.; Qin, W. Influence of Salinity and Water Content on Soil Microorganisms. *Int. Soil Water Conserv. Res.* **2015**, *3*, 316–323. [[CrossRef](#)]
41. Liu, X.; Zhang, Y.; Li, P.; Xiao, L. Changes in the biological “regulators” of organic carbon mineralization in silted soils of check dams as a result of wet–dry cycles. *Land Degrad. Dev.* **2023**; 1–12. [[CrossRef](#)]
42. Zhang, H.; Wu, P.; Yin, A.; Yang, X.; Zhang, M.; Gao, C. Prediction of Soil Organic Carbon in an Intensively Managed Reclamation Zone of Eastern China: A Comparison of Multiple Linear Regressions and the Random Forest Model. *Sci. Total Environ.* **2017**, *592*, 704–713. [[CrossRef](#)]
43. Li, X.; Xia, J.; Zhao, X.; Chen, Y. Effects of planting *Tamarix chinensis* on shallow soil water and salt content under different groundwater depths in the Yellow River Delta. *Geoderma* **2019**, *335*, 104–111. [[CrossRef](#)]
44. Cotrufo, M.F.; Ranalli, M.G.; Haddix, M.L.; Six, J.; Lugato, E. Soil Carbon Storage Informed by Particulate and Mineral-Associated Organic Matter. *Nat. Geosci.* **2019**, *12*, 989–994. [[CrossRef](#)]
45. Zhan, X.; Zhou, L. Colorimetric determination of dissolved organic carbon in soil solution and water environment (in Chinese). *China Environ. Sci.* **2002**, *22*, 433–437.
46. Liu, J.; Wu, P.; Zhao, Z.; Gao, Y. Afforestation on cropland promotes pedogenic inorganic carbon accumulation in deep soil layers on the Chinese Loess Plateau. *Plant Soil* **2022**, *478*, 597–617. [[CrossRef](#)]
47. Kölbl, A.; Schad, P.; Jahn, R.; Amelung, W.; Bannert, A.; Cao, Z.; Fiedler, S.; Kalbitz, K.; Lehdorff, E.; Müller-Niggemann, C. Accelerated soil formation due to paddy management on marshlands (Zhejiang Province, China). *Geoderma* **2014**, *228*, 67–89. [[CrossRef](#)]
48. Wissing, L.; Kölbl, A.; Schad, P.; Bräuer, T.; Cao, Z.-H.; Kögel-Knabner, I. Organic carbon accumulation on soil mineral surfaces in paddy soils derived from tidal wetlands. *Geoderma* **2014**, *228–229*, 90–103. [[CrossRef](#)]
49. Amini, S.; Ghadiri, H.; Chen, C.; Marschner, P. Salt-affected soils, reclamation, carbon dynamics, and biochar: A review. *J. Soils Sediments* **2016**, *16*, 939–953. [[CrossRef](#)]

50. Kleber, M.; Eusterhues, K.; Keiluweit, M.; Mikutta, C.; Mikutta, R.; Nico, P.S. Mineral-organic associations: Formation, properties, and relevance in soil environments. *Adv. Agron.* **2015**, *130*, 1–140. [[CrossRef](#)]
51. Feng, W.; Shi, Z.; Jiang, J.; Xia, J.; Liang, J.; Zhou, J. Methodological uncertainty in estimating carbon turnover times of soil fractions. *Soil Biol. Biochem.* **2016**, *100*, 118–124. [[CrossRef](#)]
52. Fertier, A.; Montarnal, A.; Truptil, S.; Bénaben, F. Carbon stabilization pathways in soil aggregates during long-term forest succession: Implications from $\delta^{13}\text{C}$ signatures. *Soil Biol. Biochem.* **2022**, *180*, 108988. [[CrossRef](#)]
53. Plaza, C.; Courtier-murias, D.; Fernández, J.M.; Polo, A.; Simpson, A.J. Physical, chemical, and biochemical mechanisms of soil organic matter stabilization under conservation tillage systems: A central role for microbes and microbial by-products in C sequestration. *Soil Biol. Biochem.* **2013**, *57*, 124–134. [[CrossRef](#)]
54. Lavalley, J.M.; Soong, J.L.; Cotrufo, M.F. Conceptualizing Soil organic matter into particulate and mineral-associated forms to address global change in the 21st century. *Glob. Chang. Biol.* **2020**, *26*, 261–273. [[CrossRef](#)]
55. Cotrufo, M.F.; Lavalley, J. Soil organic matter formation, persistence and functioning: A synthesis of current understanding to inform its conservation and regeneration. *Adv. Agron.* **2021**, *172*, 1–50. [[CrossRef](#)]
56. Cotrufo, M.F.; Wallenstein, M.; Boot, M.C.; Deneff, K.; Paul, E.A. The microbial efficiency-matrix stabilization (mems) framework integrates plant litter decomposition with soil organic matter stabilization: Do labile plant inputs form stable soil organic matter? *Glob. Change Biol.* **2013**, *19*, 988–995. [[CrossRef](#)]
57. Grandy, A.S.; Neff, J.C. Molecular C dynamics downstream: The biochemical decomposition sequence and its impact on soil organic matter structure and function. *Sci. Total Environ.* **2008**, *404*, 297–307. [[CrossRef](#)]
58. Lehmann, J.; Kleber, M. The contentious nature of soil organic matter. *Nature* **2015**, *528*, 60–68. [[CrossRef](#)] [[PubMed](#)]
59. Hartmann, M.; Six, J. Soil structure and microbiome functions in agroecosystems. *Nat. Rev. Earth Environ.* **2022**, *4*, 4–18. [[CrossRef](#)]
60. Yu, Y.; Xu, J.; Zhang, P.; Meng, Y.; Xiong, Y. Controlled Irrigation and Drainage Reduce Rainfall Runoff and Nitrogen Loss in Paddy Fields. *Int. J. Environ. Res. Public Health* **2021**, *18*, 3348. [[CrossRef](#)]
61. Zhao, M.; Running, S.W. Drought-induced reduction in global terrestrial net primary production from 2000 through 2009. *Science* **2010**, *329*, 940–943. [[CrossRef](#)]
62. Schwalm, C.R.; Anderegg, W.R.L.; Michalak, A.M.; Fisher, J.B.; Biondi, F.; Koch, G.; Litvak, M.; Ogle, K.; Shaw, J.D.; Wolf, A.; et al. Global patterns of drought recovery. *Nature* **2017**, *548*, 202–205. [[CrossRef](#)] [[PubMed](#)]
63. Humphrey, V.; Zscheischler, J.; Ciais, P.; Gudmundsson, L.; Sitch, S.; Seneviratne, S.I. Sensitivity of atmospheric CO_2 growth rate to observed changes in terrestrial water storage. *Nature* **2018**, *560*, 628–631. [[CrossRef](#)] [[PubMed](#)]
64. Tavakkoli, E.; Rengasamy, P.; Smith, E.; McDonald, G.K. The effect of cation-anion interactions on soil pH and solubility of organic carbon. *Eur. J. Soil Sci.* **2015**, *66*, 1054–1062. [[CrossRef](#)]
65. Wendt, J.W.; Hauser, S. An equivalent soil mass procedure for monitoring soil organic carbon in multiple soil layers. *Eur. J. Soil Sci.* **2013**, *64*, 58–65. [[CrossRef](#)]
66. Chaplot, V.; Smith, P. Cover Crops Do Not Increase Soil Organic Carbon Stocks as Much as Has Been Claimed: What Is the Way Forward? *Glob. Chang. Biol.* **2023**, *29*, 6163–6169. [[CrossRef](#)] [[PubMed](#)]

Disclaimer/Publisher’s Note: The statements, opinions and data contained in all publications are solely those of the individual author(s) and contributor(s) and not of MDPI and/or the editor(s). MDPI and/or the editor(s) disclaim responsibility for any injury to people or property resulting from any ideas, methods, instructions or products referred to in the content.